Petroleum Science 23 (2026) 3374–3383

Contents lists available at ScienceDirect

Petroleum Science

journal homepage: www.keaipublishing.com/en/journals/petroleum-science

Original Paper

Preparation and performance evaluation of phase change material microcapsules for smart regulation of drilling fluid temperature for marine gas hydrate reservoirs

Xin Zhao [a,b,*], Xiao-Long Zhang [a], Wen-Tuo Li [c], Yu-Jie Kang [a], Qi Geng [a,d], Zheng-Song Qiu [a], Zhi-Yuan Wang [a,b]

[a] School of Petroleum Engineering, China University of Petroleum (East China), Qingdao, 266580, Shandong, China
[b] Shandong Key Laboratory of Offshore Oil & Gas and Hydrates Development, China University of Petroleum (East China), Qingdao, 266580, Shandong, China
[c] CNOOC China Limited, Hainan Branch, Haikou, 570100, Hainan, China
[d] Oilfield Production Department, China Oilfield Services Limited, Tianjin, 300459, China

ARTICLE INFO

Article history:
Received 4 March 2025
Received in revised form
2 March 2026
Accepted 3 March 2026
Available online 6 March 2026

Edited by Jia-Jia Fei

Keywords:
Hydrate decomposition
Hydrate regeneration
Microcapsule
Drilling fluid
Binary composite PCM
Cold storage

ABSTRACT

In the drilling process of hydrates, hydrate decomposition and regeneration can cause wellbore collapse and plugging. Herein, phase change materials (PCMs) were introduced into the drilling fluids to regulate their temperature for controlling hydrate decomposition. The binary composite PCM and polymethyl methacrylate (PMMA) were used to prepare PCM microcapsules (PCMMs) by suspension polymerization. Basic characteristics of PCMM were studied, and its temperature-regulating effect, inhibitory performance on hydrate decomposition and regeneration, strength, and compatibility with drilling fluids were systematically investigated. The phase change temperature of the binary composite PCM could be regulated from 16 to 20 °C through the optimization of the ratio of dodecanol and fatty alcohol. When the ratio of dodecanol was 90%, the phase change temperature of PCMMs was 18 °C with the enthalpy of 93.9 $J \cdot g^{-1}$. In the heating process from 16 to 22 °C, 5% and 8% PCMM could smartly cool down the suspension through phase change energy storage to prolong the temperature rise time by 40% and 74%, respectively. Under the condition that the fluid temperature is from 2 °C around the seafloor to 25 °C at the bottom of the well in a simulation drilling process, in the heating period, 8% PCMM demonstrated superior efficacy compared to lecithin in prolonging the hydrate decomposition time by its cold release effect. In addition, the decrease in drilling fluid temperature was also hindered by the cold storage effect during the cooling stage, and the hydrate regeneration time was prolonged by 52.1%. Therefore, PCMM can reduce the risk of wellbore instability and plugging caused by hydrate decomposition and regeneration. Meanwhile, PCMMs exhibited good shearing strength and sealing property under alkaline conditions of drilling fluids and showed relatively minor impacts on the basic drilling fluid properties with a concentration of no more than 8%. This study offers a new method to maintain the safety of the hydrate drilling wellbore.

1. Introduction

Gas hydrates are the potential candidate for the future clean energy resources because of their global abundance and high energy density. Worldwide, more than 90% of the hydrates are found in deep-sea sediments (Li et al., 2022; Sun et al., 2023). However, the drilling operation can change the stress conditions of the formation, and the drill bit cutting rocks and the friction between drill tool and borehole wall generate a large amount of heat, consequently, the hydrates bearing in the sediments undergo decomposition (Yang et al., 2015; Li et al., 2021). The presence of water and the substantial volume of gas released from the hydrate decomposition led to the increase in the pore pressure and reduction in the formation strength, causing wellbore instability. Moreover, natural gas produced from the hydrate decomposition shows the potential to reconstitute hydrate within the low-temperature drilling fluid,

* Corresponding author.
E-mail address: zhaoxin@upc.edu.cn (X. Zhao).
Peer review under the responsibility of China University of Petroleum (Beijing).

https://doi.org/10.1016/j.petsci.2026.03.005

causing flow barriers (Yang et al., 2019; Zhao et al., 2024; Phan et al., 2025; Li et al., 2025). Therefore, hydrate decomposition is one of the significant technical problems for drilling in hydrate sediments (Wei et al., 2019; Zhang et al., 2022).

During the hydrate drilling process, the drilling fluid directly interacts with the hydrate, and the direct method to restrain the hydrate decomposition is to lower the drilling fluid temperature (Dong et al., 2023; Zhao et al., 2023). The ideal approach involves the implementation of a real-time control of the drilling fluid temperature in the entire drilling process. To achieve this, the key is to explore smart temperature-control additives for hydrate drilling conditions.

Phase change material (PCM) is a type of material that uses latent heat to store, transform, and utilize heat (Xu et al., 2018; Liu et al., 2024), thus, it shows potential application in the domains of air conditioning and refrigeration, refrigerated transportation, smart temperature-adjusting textiles, and building energy conservation (Yan et al., 2005; Shi et al., 2022; Liu et al., 2025). In the presence of PCM, a liquid–solid phase change occurs when the drilling fluid circulates in the wellbore, which is cooled down by the seawater. Once the fluid temperature increases to the phase change temperature of PCM in the wellbore, the PCM gets converted from the solid state to the liquid state to release cold energy (heat storage), and the drilling fluid cools down to slow down the temperature rise, thus inhibiting the hydrate decomposition. The temperature of the drilling fluid drops when it is circulated to the cold seawater well part, and the low-temperature condition raises the possibility of hydrate formation and regeneration in the borehole. As soon as the temperature drops to the PCM's phase change temperature, it changes from liquid to solid state releasing heat (cold storage). It can then heat the cold drilling fluid in the wellbore, raise its temperature, and prevent the hydrate formation and regeneration. This provides a new potential solution to address the drawbacks of traditional thermodynamic hydrate inhibitors (THIs) and kinetic hydrate inhibitors (KHIs).

As is well known, current deepwater drilling fluids rely on the addition of THIs to suppress hydrate formation, typically sodium chloride, methanol, and ethylene glycol. The concentration of thermodynamic inhibitors is very high, usually ranging from 10% to 50%, which comes with disadvantages such as high costs, environmental unfriendliness, and negative impacts on drilling fluid performance. Particularly when drilling in natural gas hydrate formations, high concentrations of THIs can promote hydrate dissociation, leading to severe wellbore instability. While KHIs cannot be effective under high subcooling conditions in deepwater (Maiti et al., 2021; Sun et al., 2022; Das et al., 2023). Therefore, balancing the inhibition of hydrate formation and dissociation poses a challenging dilemma in hydrate drilling operations. The smart temperature-control function of phase-change materials offers a novel approach to solving this problem. Moreover, the PCM can be recycled, as shown in Fig. 1. Therefore, the main objective of using PCMs is to enable the smart regulation of the drilling fluid temperature. It is required to develop PCMs corresponding to the required temperature, high mechanical properties, and good compatibility with drilling fluid.

However, direct addition of PCM into the drilling fluid may result in its performance degradation and environmental pollution. The abovementioned problems can be solved by encapsulating the PCM by a shell (Wang et al., 2023; Aiswarya et al., 2024), including preparing PCM microcapsules (PCMMs) and PCM composites. PCMMs are core-shell structured materials where the PCM serves as the core encapsulated by a wall material. They exhibit excellent stability and leakage-proof performance, but demonstrate poor mechanical strength, particularly under high-temperature conditions. Therefore, they are more suitable for

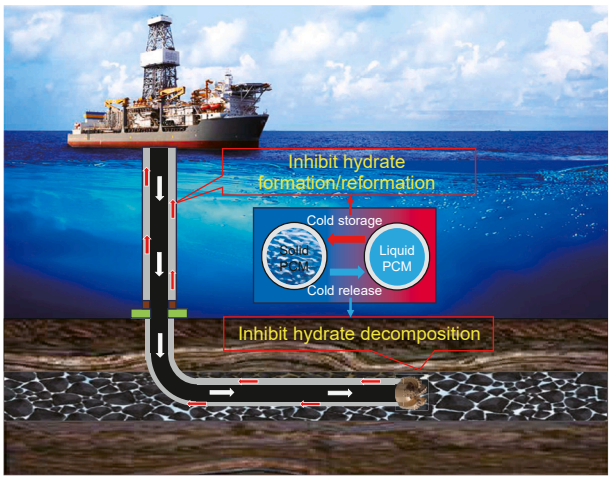

Fig. 1. Principle diagram of control of drilling fluid temperature by PCMs.

dynamic applications such as drilling fluids, cement slurries, and engineered thermal fluids (Nazir et al., 2018; Zhao et al., 2023). In contrast, PCM composites are fabricated by directly dispersing or adsorbing the PCM into a porous matrix, and they offer simpler preparation and higher mechanical strength. However, they carry a greater risk of core material leakage than PCMMs. Therefore, they have been studied for building energy conservation. For example, to enhance the thermal insulation performance of the wall, Shi et al. (2020) investigated the thermal and mechanical properties of thermal energy storage lightweight aggregate mortar incorporated with PCM. Liu et al. (2025) prepared the composite cenosphere-based PCM composed of PCM and acid-modified cenosphere to produce a novel foam geopolymer concrete. To avoid the rupture of microcapsule or the leakage of the core material, it is required for the shell material of microcapsule to have sufficient mechanical strength and sealing property when the drilling fluid circulates in the well. Studies have shown that polymethyl methacrylate (PMMA) is a type of wall material with high strength. For example, Zhao et al. (2017) prepared n-octadecane@PMMA microcapsules which showed potential application value in smart temperature control in the textile industry. Meng et al. (2020) prepared paraffin wax@PMMA microcapsules as thermal insulation materials in the construction industry, and the experimental results revealed their advantages of stable shape, no leakage, and good reliability.

According to the formation conditions of hydrates, the drilling fluid temperature ought to be regulated within 20 °C to prevent hydrate decomposition. Considering the characteristics of practical application, a buffer interval of 2 °C is reserved, thus it is necessary to prepare PCM microcapsule with a phase change temperature of 18 °C. However, unfortunately, the fixed phase change temperature of currently used PCMs cannot fully meet the requirements. Therefore, with reference to the methods employed in the fields of air conditioning refrigeration, refrigerated transportation, and smart temperature-adjusting textiles, two or more PCMs can be prepared into eutectic PCMs by physical methods such as melt blending, and the overall phase change temperature can be regulated via modifying the proportion of each component (Nazir et al., 2018). This strategy offers theoretical guidance for the research and development of PCMM that can meet the drilling fluid temperature requirements in marine hydrate formation.

In this study, core with the phase change temperature of about 17.8 °C was prepared via optimizing the dodecanol/fatty alcohol binary composite PCM, and the PCMMs were prepared by using PMMA

as the shell material to wrap the composite core material. Next, the comprehensive performance evaluation was carried out. Smart temperature control approach for drilling fluid by utilizing PCMM is expected to provide a new strategy for wellbore stability as well as hydrate formation inhibition during hydrate drilling in the sea area.

2. Materials and methods

2.1. Materials

Dodecanol, fatty alcohol, sodium hydroxide (NaOH), ethanol, and sodium lauryl sulfate (SDS) were purchased from Macklin Biochemical Technology Co., Ltd. Methyl methacrylate (MMA) and pentaerythritol tetraacrylate were procured from Shanghai Aladin Biochemical Technology Co., Ltd. Azobisisobutyronitrile (AIBN) and the emulsifier were supplied by Sinopharm Chemical Reagent Co., Ltd. Xanthan gum (XC) was supplied by Ordos Zhongxuan Biochemical Co., Ltd.

2.2. Methods

2.2.1. Fabrication of binary composite phase change material

Based on the requirement of inhibiting hydrate decomposition for drilling through hydrates in the South China Sea, this study aims at preparing core with phase change temperature of about 18 °C so that when the fluid temperature exceeds its melting temperature, the PCM wrapped in the shell undergoes phase change to release cold, leading to the delayed rise in the fluid temperature. Based on the second law of thermodynamics and phase equilibrium theory, Eqs. (1) and (2) were derived to predict the phase change temperature and enthalpy of different PCMs combinations (Zhang et al., 1995). Through theoretical calculations, dodecanol and another fatty alcohol were selected as the monomers for the binary composite PCM. The ratio of the binary composite was subsequently optimized. First, dodecanol and another fatty alcohol were mixed in proportion, following which the mixture was heated and melted in a constant temperature bath at 55 °C for 1 h. Next, the mixture was continuously stirred, and ultrasonically vibrated for about 40 min to assure uniform dispersion of the mixture. Finally, the mixture was cooled down to obtain the binary composite PCM.

$$T_{\mathrm{m}} = \frac{H_i T_i}{H_i - T_i R \ln x_i} \tag{1}$$

$$H_{\mathrm{m}} = T_{\mathrm{m}} \sum_{i=A,B} \frac{x_i H_i}{T_i} \tag{2}$$

where, T_{m} represents phase change temperature of the composite PCM (°C), H_{m} denotes phase change enthalpy of the composite PCM (J/g), T_i indicates phase change temperature of substances A and B (°C), H_i represents latent heat of fusion for substances A and B (J/mol), R is the gas constant (8.314 J/(mol·K)), x_i denotes molar fraction of substances A and B ($x_A + x_B = 1$).

2.2.2. Performance evaluation of binary composite phase change materials

(1) Step-cooling curve test

The prepared binary composite PCMs with different proportions of dodecanol and fatty alcohol were placed in a thermostatic water tank at 25 °C and allowed to stand until they were fully melted. Then, they were quickly placed in a thermotank at 8 °C to simulate the change in drilling fluid temperature from the platform to the well bottom during the drilling process. A temperature sensor was used to record the temperature change over time. Data were collected every minute until the temperature of the PCM in the incubator stabilized, and after the completion of the experiment, a step-cooling curve of the binary composite PCM with different proportions was drawn according to the test results, and the phase change temperature was analyzed.

(2) Differential scanning calorimetry test

Differential scanning calorimetry (DSC) was utilized to measure the melting temperature and latent heat of binary composite PCM using a 214 polyma differential scanning calorimeter. The flow rate was 35 mL·min^{-1}, and the temperature was increased from 10 to 30 °C at a rate of 2 °C·min^{-1}.

(3) Cycle stability test

The binary composite PCMs were repeatedly put into the environment of 25 and 8 °C, and the heating–cooling operation was cycled for 20 times. The first and twentieth heating and cooling cycle data were recorded, the step-cooling curve was drawn, and the cycle stability of the binary composite material was analyzed.

2.2.3. Preparation of PCMM

Suspension polymerization method was employed to prepare PCMM utilizing PMMA as the wall and binary composite PCM as the core, as shown in Fig. 2. The detailed procedure is as follows: (1) 5 g of the wall material monomer MMA and the composite core material were weighed into a beaker at room temperature. The initiator AIBN and the cross-linking agent pentaerythritol tetraacrylate were then added, and the mixture was subjected to ultrasonic dispersion to obtain an oil phase. (2) A specific amount of deionized water was weighed, and a small quantity of emulsifier was added. The oil phase was slowly incorporated while stirring at a speed of 2000 r·min^{-1} to prepare an emulsion. (3) Next, this emulsion was put into a three-necked flask, which was moved into a thermostatic water bath while nitrogen was introduced into the flask. After stirring and allowing the reaction to proceed, the product was cooled down, washed, filtered, and dried to yield PCMM.

2.2.4. Structural characterization of PCMM

A Nexus-870 Fourier transform infrared (FTIR) spectrometer was used to test the IR spectrum of the microcapsules. A SU8010 scanning electron microscopy (SEM) was used to characterize the morphology of the microcapsules, and a Bettersize 2000 laser particle size analyzer was used to measure the distribution of particle sizes of the microcapsule.

2.2.5. Performance evaluation of PCMM

(1) Phase change characteristic test

For analyzing the phase transition characteristics of PCMM during the heating procedure, DSC was employed to test the phase change temperature and enthalpy of microcapsules from 10 to 30 °C.

(2) Phase change temperature control effect test

Aqueous solution of XC (0.1%) was prepared, and PCMM sample (0%, 5%, and 8%, respectively) was added. The process of increase in temperature of three groups of samples from 15 to 25 °C was

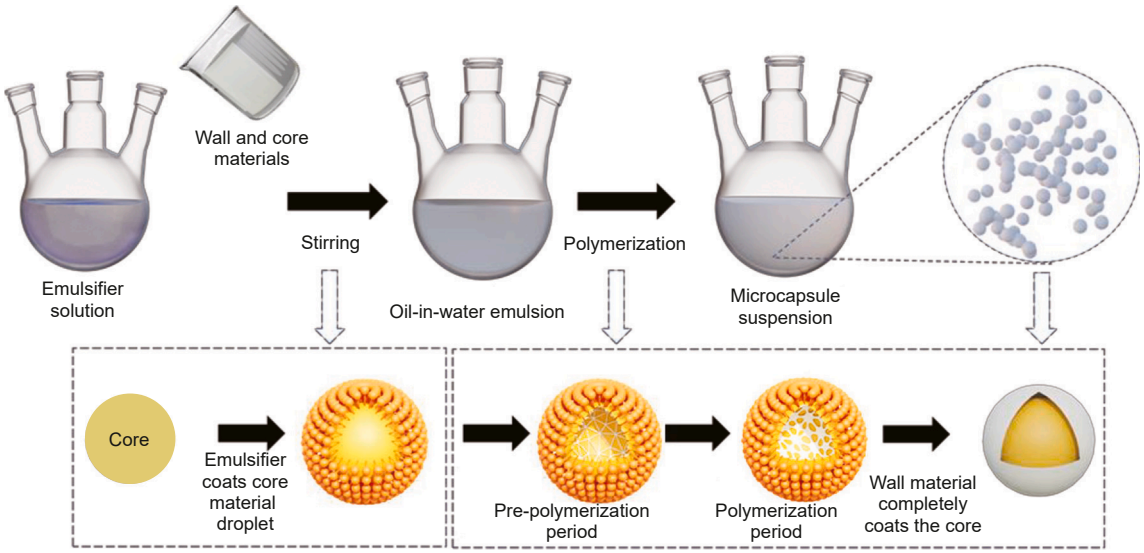

Fig. 2. Schematic illustration of preparation process of PCMM.

simulated in an incubator, and the temperature of liquid phase was recorded in real time using a temperature sensor. Next, the temperature-time curve of each sample was plotted during the temperature rise process.

(3) Hydrate decomposition and regeneration inhibition performance

By using the self-made experimental device of drilling fluid for marine hydrate drilling (Zhao et al., 2019), the circulation process of drilling fluid was simulated (Yin et al., 2025), and the process of cold storage, cold release, and cold storage of PCM was realized. The decomposition and regeneration of hydrate in XC solution (0.1%), XC solution (0.1%) with lecithin (0.5%), and XC solution (0.1%) with PCMM (8%) were compared and analyzed. The main experimental steps are as follows: SDS solution (concentration: 0.0025%) was injected into a high-pressure autoclave, the temperature was reduced to 2 °C, the pressure was increased to 12 MPa by injecting methane, and the data of temperature and pressure in the reaction kettle were recorded at the moment. When the pressure and temperature stabilized and the hydrate generation process was completed, the refrigeration system was shut down. Then, the test solution that had been cooled down to 2 °C, was pressed into the reaction kettle through the displacement system. The water bath temperature was set to 25 °C to increase the reaction kettle temperature subsequently, which resulted in commencing the hydrate decomposition. After 3 h, the thermostatic bath temperature was reset to 2 °C. With the decrease in the temperature of the autoclave, favorable conditions were provided for the formation of hydrate. After 10 h, the data recording was stopped, the pressure in the kettle was released, and the experiment ended. Based on the temperature and pressure changes in the reaction kettle, Peng-Robinson equation (Eq. (3)) (Zhao et al., 2019) was introduced for calculating the change in the mole number of methane during the experiment, and the influence of PCMMs on hydrate decomposition and regeneration characteristics was analyzed.

$$P = \frac{RT}{V_m - b} - \frac{a(T)}{V_m(V_m + b) + b(V_m - b)} \tag{3}$$

where P represents pressure (MPa), T denotes temperature (K), V_m indicates molar volume ($L \cdot mol^{-1}$), R denotes the gas constant, and the energy $a(T)$ can be determined by using the critical parameters. Further, b, the co-volume constant, can be determined from the eccentric factor.

(4) Strength test of phase change microcapsules

The microcapsules were added into NaOH solutions with pH values of 7, 10, 11, and 12, respectively, and stirred for 30 min using a high-speed shearing machine at a certain shearing rate (2000, 4000, 6000, 8000, and 10,000 $r \cdot min^{-1}$). PCMMs were then washed with absolute ethyl alcohol, filtered, dried, and their residual mass was weighed. According to Eq. (4), the damage rate of the microcapsule under different shear rates was calculated, which can be used to characterize the strength of the microcapsule under the condition of high-speed shear of drilling fluid, and to analyze the probability of damage in drilling operation.

$$\varepsilon = \frac{C - D}{C\alpha} \times 100\% \tag{4}$$

where ε stands for the damage rate of PCMM (%), C and D are the original and final mass of PCMM, respectively (g), and α denotes the coating rate of the microcapsule (%). The PCMM was ultrasonically crushed in absolute ethyl alcohol using an ultrasonic cell crusher, and the ratio of the mass difference to the initial mass before and after crushing was calculated.

(5) Sealing test of microcapsules

By testing the long-term sealing performance of microcapsules, the risk of slow leakage of the core material caused by the insufficient sealing property of the wall material was analyzed in this study. A certain mass of PCMM was added into four NaOH solutions with pH values of 7, 10, 11, and 12, respectively, and their suspensions were prepared. Next, the suspensions were stirred at a low speed (200 $r \cdot min^{-1}$) for 1, 3, 7, and 15 d, respectively. Further, they were washed, filtered, and dried with absolute ethanol. The remaining mass was then weighed, and the lost mass

corresponded to the leaked core mass. Finally, the core loss rate was calculated by using Eq. (4), which represents the precipitation ratio of the core material.

(6) Evaluation of compatibility

To exhibit excellent compatibility with the drilling fluid, PCMM should not have any significant adverse effects on the drilling fluid properties. The rheology and filtration tests were performed at 25 and 2 °C using the drilling fluid with 5% and 8% PCMM to assess their compatibility.

3. Results and discussion

3.1. Experimental results of property evaluation of binary composite PCMs

3.1.1. Step-cooling curve

The step-cooling curves and phase change temperatures of six groups of PCM samples with different mass ratios of dodecanol to fatty alcohol are shown in Figs. 3 and 4. The findings suggest that with the increase in the dodecanol content, the PCM phase change temperature first decreases and then increases. Considering that the required PCM phase change temperature is about 18 °C, when the mass percentage of dodecanol amounted to 78% and 90%, the core phase change temperature was about 17.6 °C, which meets the requirements. However, the latent heat of dodecanol is higher than that of fatty alcohol; therefore, the composite PCM with 90% dodecanol mass fraction was selected as the core material.

3.1.2. Differential scanning calorimetry test results

Fig. 5 presents the DSC results of PCM when the mass percentage of dodecanol was 90%. The results reveal that for the 90% mass ratio of dodecanol, the melting temperature is 17.8 °C, which is in line with the test results of the step-cooling curve presented in Section 3.1.1. The peak melting temperature is 19.6 °C, and the latent heat is 182.2 $J \cdot g^{-1}$. Moreover, the DSC curves show the presence of only one phase change peak in the melting course of the binary composite PCM with dodecanol mass percentage of 90%, which indicates that no phase separation occurs for the composite made of the two materials.

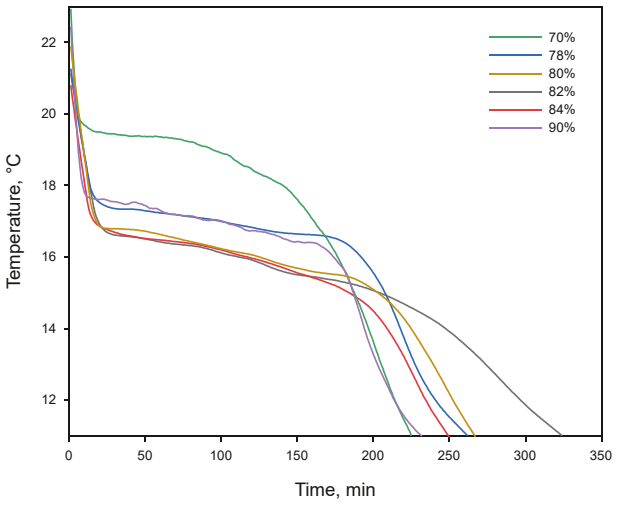

Fig. 3. Step-cooling curves of PCMs with different dodecanol content.

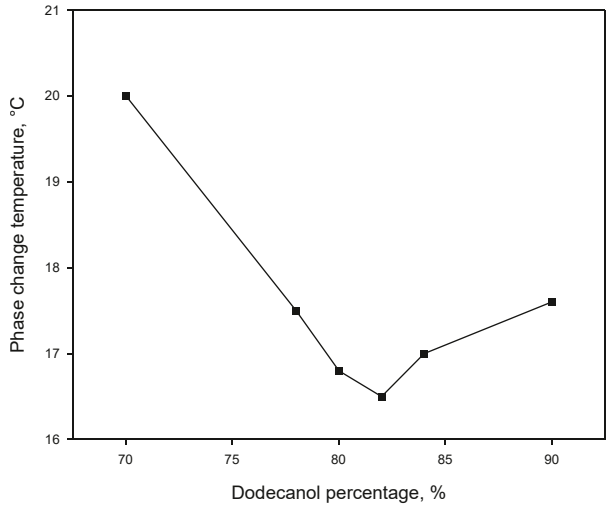

Fig. 4. Phase change temperature of composite PCMs with different dodecanol mass percentage.

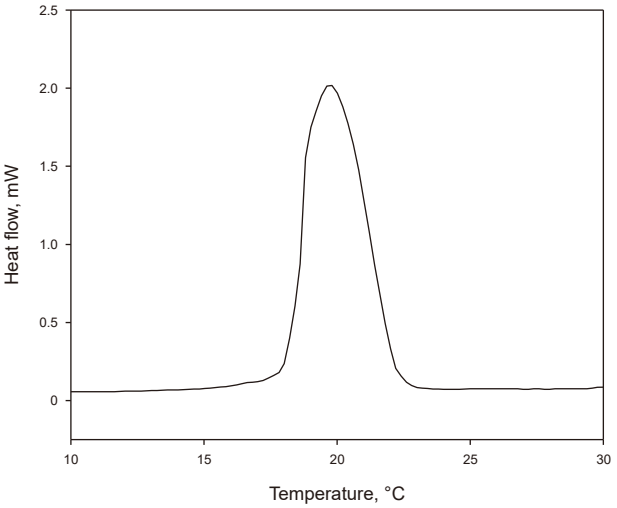

Fig. 5. DSC curve of binary composite PCM with dodecanol mass fraction of 90%.

3.1.3. Cycle stability

The step-cooling curves of binary composite PCMs with different proportions after 20 heating–cooling cycles are shown in Fig. 6. The experimental results indicate that the phase change temperature of PCM remained almost unchanged compared with the initial state after 20 times of thermal cycling. This result suggests that the phase transition features of the composite PCMs were stable after multiple cycles, which could meet the needs of microcapsule recycling.

3.2. Characterization of PCMM

3.2.1. Morphological characteristics and particle size distribution

Figs. 7 and 8 show the SEM images and particle size of the prepared PCMMs. Fig. 7(a) evidently presents that the microcapsule has a spherical shape, the wall material is comparatively dense, and the wrapping effect is good. Fig. 7(b) shows that a few ruptured microcapsules were formed during the preparation process, clearly revealing their capsule structure consisting of a wall material shell and the enclosed core substance. According to the results of particle

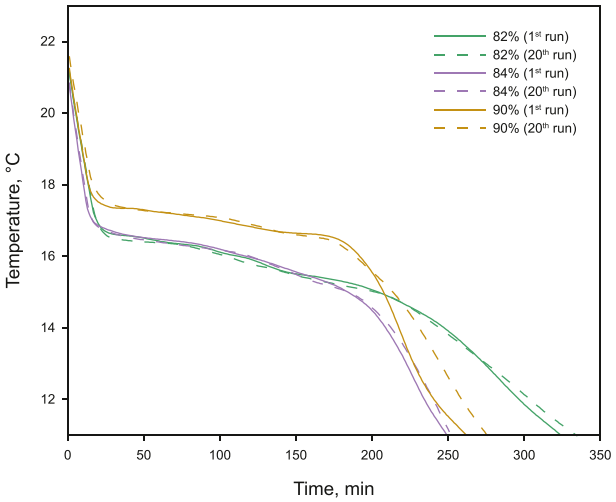

Fig. 6. Step-cooling curves of PCMs with different mass fractions of dodecanol after multiple cycles.

size test, PCMMs produced via suspension polymerization exhibited a uniform particle size distribution, mainly in the interval of 1–10 μm, and the D_{50} value equaled 3.9 μm.

3.2.2. Chemical structure analysis

Fig. 9 shows FTIR spectra of MMA, binary composite core material, and PCMM. The FTIR spectrum of the wall material MMA exhibits an absorption peak at 1719.99 cm^{-1}, which corresponds to an unsaturated elongation vibration of –C=O group, and the peak at 1195.84 cm^{-1} indicates tensile vibration of –C–O. The FTIR spectrum of the binary composite core material shows the peaks at 3347.71, 2921.26, and 2852.48 cm^{-1}, which can be ascribed to the elongation vibration of –OH, $–CH_2$, and $–CH_3$ groups, respectively. The absorption peak at 1465.93 cm^{-1} is attributed to the scissoring vibration of $–CH_2$, the absorption peak at 1054.91 cm^{-1} corresponds to the stretching vibration of –C–O, and the absorption peak at 721.02 cm^{-1} is due to the in-plane rocking vibration of $–CH_2$, which correspond to the signature absorption peaks of the composite core material. In the FTIR spectrum of PCMM, compared with the wall material MMA, the peaks at 1719.99 and 1195.84 cm^{-1} still exist, and the characteristic absorption peaks appear at 3347.71, 1054.91, and 721.02 cm^{-1} for the composite core material. The results show that the prepared PCMM is composed of MMA wall material and composite core material, and the core is compatible with shell materials.

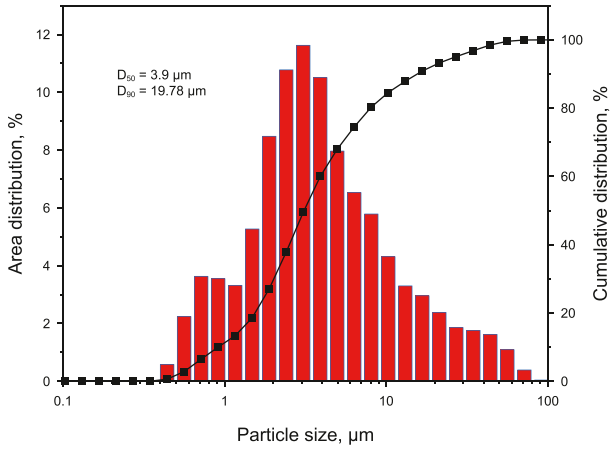

Fig. 8. Particle size distribution of PCMMs.

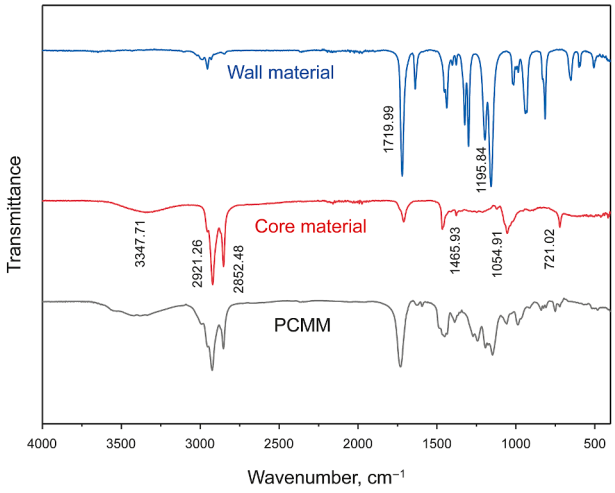

Fig. 9. FTIR spectra of wall material, core material, and PCMM.

3.3. Performance evaluation of PCMM

3.3.1. Phase change characteristics

Fig. 10 shows DSC result of the melting process of PCMM core material in the course of heating. The melting temperature of the prepared PCMM is 18 °C, which is in line with the DSC test findings

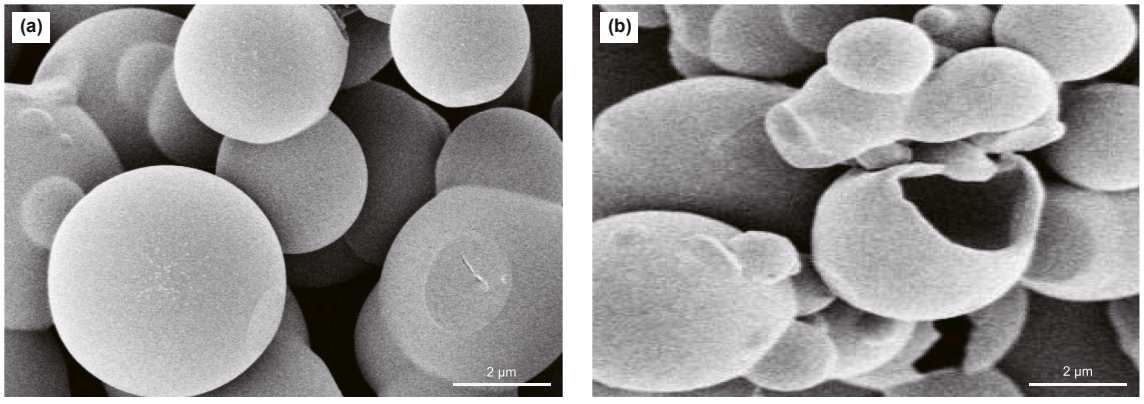

Fig. 7. SEM image of PCMMs.

of the core material presented in Section 3.1.2. The peak temperature of phase change is 19.9 °C, that is, the core material begins to melt when the drilling fluid temperature exceeds 18 °C, and gradually releases cold energy to play a role in cooling, so as to avoid or delay the fluid temperature rise to the hydrate decomposition temperature. The enthalpy value of phase change is high, that is 93.9 $J \cdot g^{-1}$, which can ensure good phase change temperature control efficiency.

3.3.2. Phase change temperature control performance

Fig. 11 shows the temperature-time curve during the heating process with 0.1% XC solution and added 5% and 8% phase change microcapsules, respectively. The starting test solution temperature was fixed at 16 °C, and the test solution temperature required 53 min to increase from 16 to 22 °C without adding microcapsules. After the addition of PCMM, the suspension shows an obvious temperature step at 18–20 °C because of the release of cold energy during its phase change. Moreover, the time for the suspension to heat up to 22 °C extends to 74 and 92 min by using 5% and 8% PCMM, respectively, that is, the heating time is respectively prolonged by 40% and 74%. The results show that the PCMM can significantly delay the temperature rise of the suspension through phase change.

3.3.3. Hydrate decomposition and regeneration inhibition performance

During hydrate drilling, the fluid temperature rise causes hydrate decomposition, and the time for the produced gas and water to regenerate hydrate is shorter than that for the first generation of hydrate, which is called “Memory Effect” (Parent and Bishnoi, 1996; Takeya et al., 2000). Therefore, the gas generated by hydrate decomposition is more likely to again produce hydrate in the wellbore, resulting in wellbore plugging. Fig. 12 shows a graph comparing pressure, temperature, during hydrate decomposition and regeneration in a 0.1% XC solution, 0.1% XC solution with 0.5% lecithin, and a 0.1% XC solution with 8% PCMM.

As illustrated in Fig. 12(a–c), during the heating phase, compared to the 0.1% XC solution, the addition of 0.5% lecithin to the 0.1% XC solution extended the hydrate decomposition time from 2.5 to 2.8 h. Under identical conditions, PCMM further prolonged the decomposition time from 2.5 to 3.0 h. Mechanistically, lecithin inhibited hydrate dissociation by adsorbing onto the hydrate surface via its choline groups and methyl-functionalized

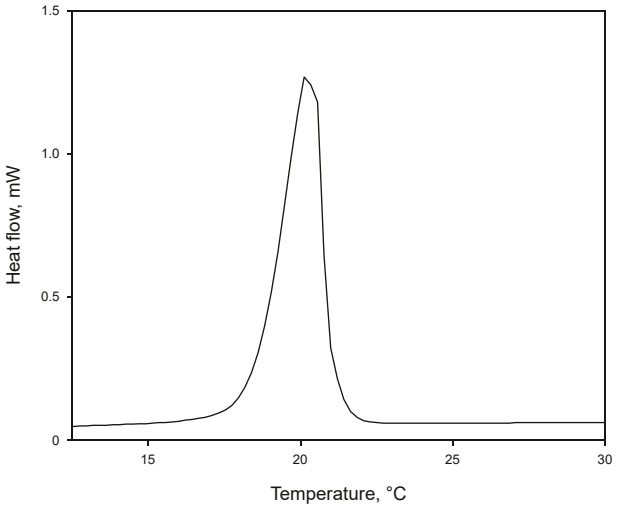

Fig. 10. DSC curve of PCMM.

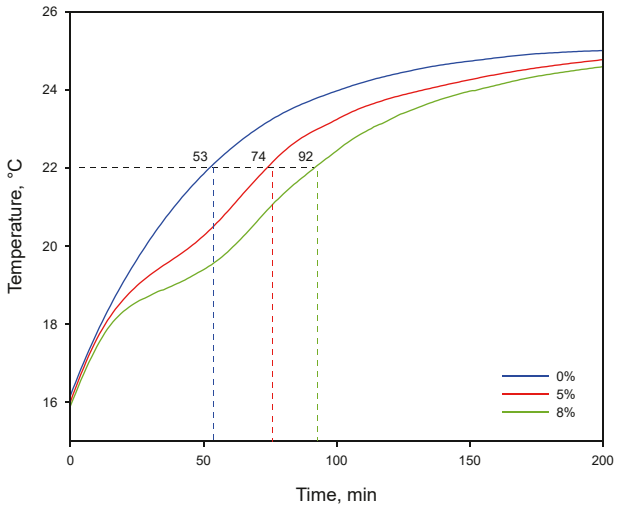

Fig. 11. Temperature-time curves of PCMM suspension.

fatty acid chains. This adsorption delays heat transfer, mitigates structural disruption of the hydrate clathrate framework, and prevents methane escape (Chen et al., 2025). Compared to lecithin, PCMM suppressed hydrate decomposition by delaying the temperature rise in the autoclave through its phase-change cooling effect. Fig. 13 exhibits a temperature comparison curve of the hydrate decomposition and regeneration processes in the three groups of samples, and Fig. 14 presents a comparative analysis of methane release or consumption using the Peng-Robinson equation. Fig. 13 indicates that lecithin did not alter the temperature in the autoclave, resulting in a temperature profile that nearly overlaps with that of the 0.1% XC solution. In comparison, the phase-change cooling effect of the PCMM extended the time required for the system to heat up from the initial temperature to 25 °C by 0.5 h (from 2.3 to 2.8 h). Fig. 14 demonstrates that lecithin reduced the maximum instantaneous methane release from hydrate decomposition by 0.15 mol at the same time point, while the PCMM achieved a significantly higher reduction of 0.39 mol due to its phase-change cooling effect.

Notably, during the cooling phase, compared to the 0.1% XC solution, lecithin shortened the hydrate formation time from 4.8 to 4.4 h, failing to exhibit inhibition effects and even promoting hydrate reformation, thereby increasing the risk of blockages. In contrast, PCMM extended the time required for the system to cool from 25 °C to the same temperature by 0.7 h (from 4.9 to 5.6 h) through its phase-change cold storage capacity. Additionally, PCMM prolonged the hydrate formation time from 4.8 to 7.3 h and reduced the maximum instantaneous methane consumption for hydrate formation by 0.4 mol at the same time. Thus, PCMM demonstrates superior efficacy in inhibiting hydrate generation compared to lecithin.

The effect of PCMM on inhibiting hydrate regeneration in the cooling stage is more obvious than the effect on inhibiting hydrate decomposition in the heating stage. Notably, when the microcapsules release heat during phase change, they may cause the residual methane dissolved in water produced during hydrate decomposition to be released. These bubbles remaining in the water produced by hydrate decomposition are an important reason for shortening the induction period of hydrate regeneration (Uchida et al., 2016; Zhang et al., 2018). Therefore, the “Memory Effect” of secondary formation of hydrate gets weakened, and the induction period of secondary formation of hydrate is prolonged. Moreover, Fig. 12(a–c) clearly reveal that the pressure drop is

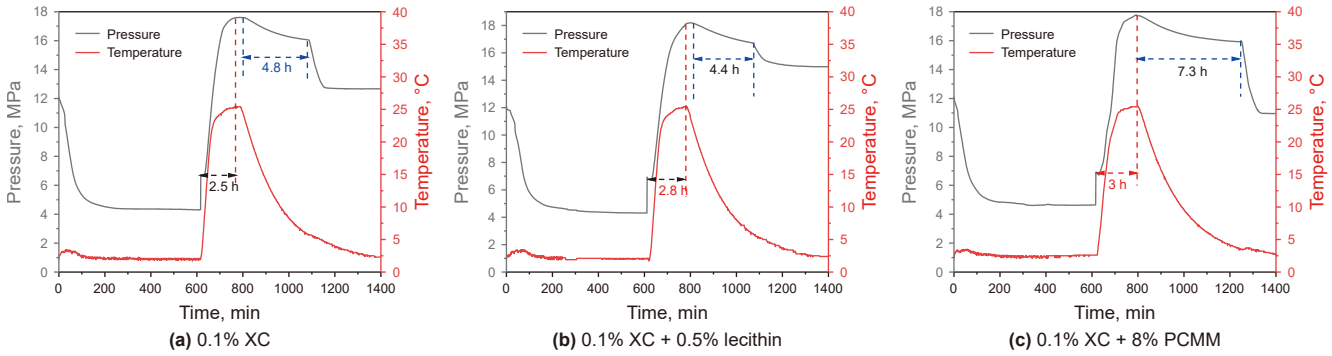

Fig. 12. Comparison curves of temperature, pressure in the course of hydrate decomposition and regeneration when injecting different test solutions.

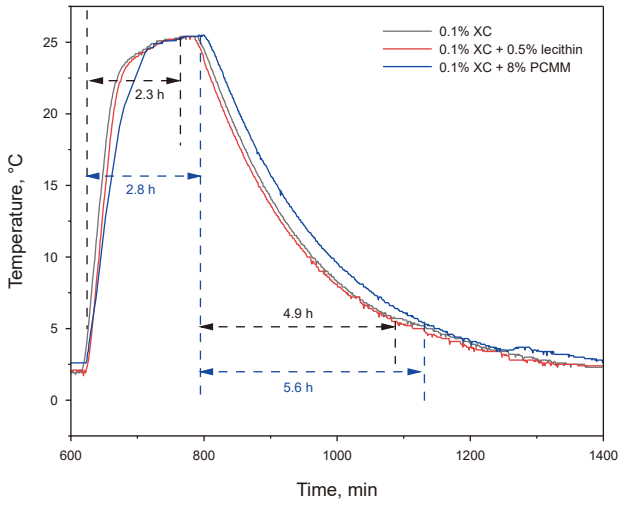

Fig. 13. Comparison curves of temperature in the course of hydrate decomposition and regeneration when injecting different test solutions.

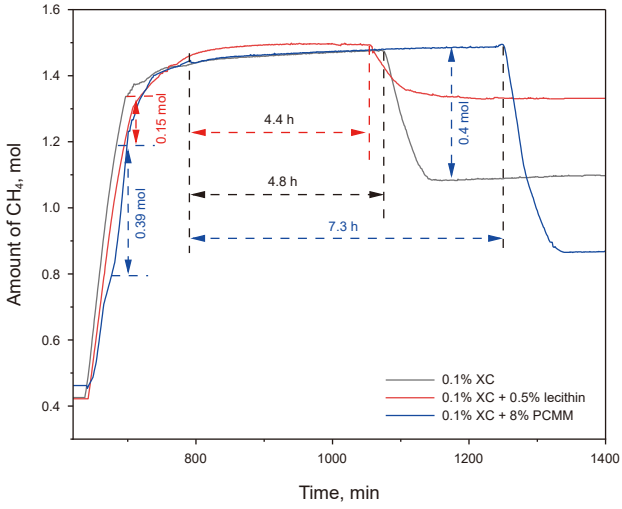

Fig. 14. Comparison curves of methane release or consumption in the course of hydrate decomposition and regeneration when injecting different test solutions.

divided into two stages after the temperature drop starts at 800 min. The pressure drop in the first stage may be caused by the re-dissolution of methane released by hydrate decomposition in water (mainly water produced by hydrate decomposition). Compared with Fig. 14, it is observed that no hydrate is produced during the first stage, while decrease in the autoclave pressure during the second phase is caused by the formation of copious hydrate.

The above-mentioned experimental results indicate that the PCMM prepared in this study exhibits good performance of inhibiting hydrate decomposition and regeneration, which is conducive to reducing the risk of wellbore instability caused by hydrate decomposition and wellbore plugging caused by hydrate regeneration in marine natural gas hydrate drilling.

3.3.4. *Strength of microcapsule wall material*

(1) Shear resistance

Fig. 15 shows the PCMM breakage rate at various centrifugal shear rates in different pH environments. The results show that the wall materials of some PCMMs were broken by high-speed stirring and shearing, and the breakage rate of PCMM increased with increasing shear rate. At 10,000 r·min^{-1}, the breakage rate was 8%, and the PCMM exhibited good shear strength. Notably, as the pH increased, the mass loss curves of PCMMs showed negligible deviation from those at a pH value of 7, demonstrating that PCMMs maintain excellent shear resistance under alkaline conditions of drilling fluids, even at a pH value of 12.

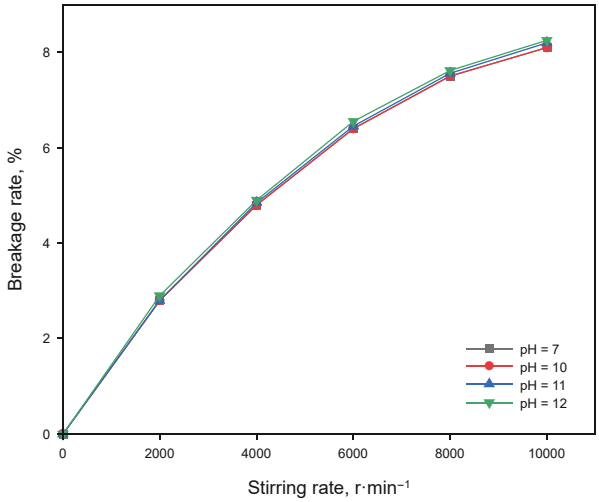

Fig. 15. Damage rate of PCMM at different shear rate.

(2) Sealing performance

Fig. 16 shows the loss of the core material after the PCMMs were stirred at 200 r·min^{-1} in different pH environments for 1, 3, 7, and 15 d, respectively. After stirring for 1 d, a small amount of PCMM with poor sealing property quickly leaked from the core, and the loss rate of the core became approximately 3%. With the time prolongation, the core precipitation ratio increased slowly, and the core loss rate of PCMM was about 7% after stirring for 15 d. Notably, as the pH increased, the core material loss rate remained nearly identical to that observed at pH = 7. Therefore, the PCMMs developed in this work demonstrate excellent sealing performance under the high-pH environments of drilling fluids.

3.3.5. Compatibility of PCMM with drilling fluid

After adding 5% and 8% PCMM to the formula of water-based drilling fluid (4% Bentonite + 0.2% NaOH + 0.1% XC + 0.5% JLS-2 + 0.5% PAC-LV) for deepwater drilling, the pH was adjusted to 10 using NaOH. The rheological and filtration parameters are displayed in Table 1. When PCMMs were added, the solid content in the drilling fluid increased. Consequently, the plastic viscosity increased slightly, the yield point remained basically unchanged, and the filtration loss dropped slightly. At 2 °C, after adding 5% and 8% PCMM, respectively, the apparent viscosity increased by 8.3% and 15.6%, separately, while the fluid loss decreased by 8.3% and 9.7%. Therefore, the addition of PCMMs with a concentration of no more than 8% could slightly increase the viscosity of drilling fluid, but did not cause serious thickening. It slightly improved the filtration and wall building of drilling fluid, indicating that the developed PCMM is highly compatible with drilling fluid.

The aforementioned experiments confirm that incorporating PCMs into drilling fluids, leveraging their phase transition-based cold storage and release capabilities, can achieve a certain degree of smart cooling of drilling fluids. To fully explore the application potential of PCMs in drilling fluids, future research can be pursued in the following aspects. (1) In light of the cooling requirements for drilling fluids in operations involving special formations such as low-temperature hydrate formations and deep high-temperature formations, explore high latent heat PCMs suitable for different temperature ranges to achieve efficient and smart cooling of downhole drilling fluids. (2) Further investigate methods to enhance the strength, stability, and thermal conductivity of wall materials to better meet the application demands in high-pressure and high-shear environments encountered in drilling operations. (3) Explore low-cost PCMs or PCMMs to meet the cost control requirements for industrial applications.

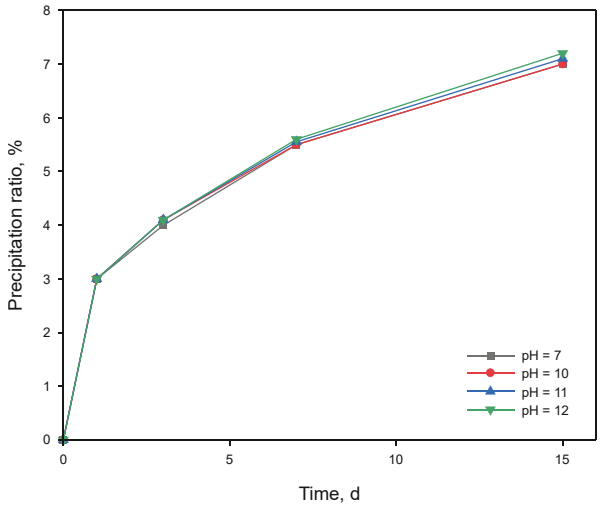

Fig. 16. Permeation curve of PCMM.

Table 1
Experimental results of compatibility between PCMM and water-based drilling fluid.

No.	Temperature, °C	AV, mPa·s	PV, mPa·s	YP, Pa	Gel, Pa/Pa	FL, mL	pH
1#	25	34	18	16	14/21	8.0	10
	2	48	27	21	16/25	7.2	10
2#	25	37.5	21	16.5	17/24	7.8	10
	2	52	31	21	19/26	6.6	10
3#	25	39	23	16	18/25	7.6	10
	2	55.5	34	21.5	20/27	6.5	10

4. Conclusions

(1) According to the drilling fluid temperature control requirements in the hydrate formation, the phase change temperature of the core was effectively controlled from 16 to 20 °C through the optimization of the ratio of dodecanol and fatty alcohol binary composite core material, and it remained stable during cyclic use. PCMM with a phase change temperature of 18 °C was prepared by using a composite material with 90% dodecanol as the core and PMMA as the shell.

(2) The PCMM can delay the increase in drilling fluid temperature through the cold storage–release effect, and the PCMMs with the concentration of 5% and 8% can prolong the temperature rise time of the suspension from 16 to 22 °C by 40% and 74%, respectively, which exhibits a certain smart temperature control effect.

(3) Under the condition that the fluid temperature is from 2 °C around the seafloor to 25 °C at the bottom of the well in a simulation drilling process, the PCMM can restrain the hydrate decomposition in the fluid temperature rising process and the hydrate regeneration in the temperature falling process through the temperature regulation function, and demonstrates superior efficacy compared to lecithin, the typical hydrate dissociation inhibitor. Therefore, in hydrate drilling operation, PCMM is conducive to alleviating wellbore instability resulting from hydrate decomposition and the wellbore blockage risk caused by hydrate regeneration. It provides a new idea for preventing wellbore instability and wellbore plugging during hydrate drilling to ensure wellbore safety.

(4) The prepared PCMMs exhibit good shearing strength and sealing property under alkaline conditions of drilling fluids, which avoids the large-area rupture of PCMMs and the leakage of the core material in drilling operations.

(5) PCMMs with a concentration of no more than 8% show relatively minor impacts on the basic drilling fluid properties, indicating that PCMMs possess good compatibility with drilling fluids, ensuring its applicability in the drilling fluids for offshore natural gas hydrate exploration.

CRediT authorship contribution statement

Xin Zhao: Writing – original draft, Investigation, Conceptualization. **Xiao-Long Zhang:** Writing – review & editing, Investigation, Formal analysis. **Wen-Tuo Li:** Methodology. **Yu-Jie Kang:** Investigation, Data curation. **Qi Geng:** Methodology, Investigation. **Zheng-Song Qiu:** Supervision, Project administration, Funding acquisition. **Zhi-Yuan Wang:** Supervision.

Declaration of competing interest

The authors declare that they have no known competing financial interests or personal relationships that could have appeared to influence the work reported in this paper.

Acknowledgments

This work was supported by the Oil & Gas Major Project of China (2025ZD1403200), the National Natural Science Foundation of China (52474024), and the Fundamental Research Funds for the Central Universities (25CX02026A).

References

Aiswarya, V., Das, S., Watmode, P.D., Gajghate, S.S., 2024. Development of hybrid MgO/GO modified microencapsulated phase change material for thermal energy management: An experimental approach. J. Clean. Prod. 434, 140399. https://doi.org/10.1016/j.jclepro.2023.140399.

Chen, D., Miao, T., Chang, C., Guo, X., An, M., Guan, M., Ji, Z., 2025. Molecular insights into inhibition and manipulation of methane hydrate dissociation by lecithin and poly (N-vinylpyrrolidone). Fuel 381, 133580. https://doi.org/10.1016/j.fuel.2024.133580.

Das, S., Mahto, V., Udayabhanu, G., Lall, M.V., Singh, K., Deepak, M., 2023. Evaluation of L-ascorbic acid as a green low dosage hydrate inhibitor in water-based drilling fluid for the drilling of gas hydrate reservoirs. J. Pet. Sci. Eng. 220, 111156. https://doi.org/10.1016/j.petrol.2022.111156.

Dong, L., Wu, N., Leonenko, Y., Wan, Y., Liao, H., Hu, G., Li, Y., 2023. A coupled thermal-hydraulic-mechanical model for drilling fluid invasion into hydrate-bearing sediments. Energy 278, 127785. https://doi.org/10.1016/j.energy.2023.127785.

Li, C., Pei, J.L., Wu, N.H., et al., 2022. Rotational failure analysis of spherical-cylindrical shell pressure controllers related to gas hydrate drilling investigations. Pet. Sci. 19, 789–799. https://doi.org/10.1016/j.petsci.2022.02.005.

Li, E., Wang, Z.Y., Zhang, Y., Guo, Y.K., Li, P.F., Zhang, J.B., Kong, Q.W., 2025. Microscopic forces between methane hydrate particle and droplet-wetted sand grain surface in a high-pressure system: experiments and mechanisms. Pet. Sci. https://doi.org/10.1016/j.petsci.2025.11.042.

Li, Y., Liu, L., Jin, Y., Wu, N., 2021. Characterization and development of natural gas hydrate in marine clayey-silt reservoirs: A review and discussion. Adv. Geotherm. Energy Res. 5, 75–86. https://doi.org/10.46690/ager.2021.01.08.

Liu, Y., Zhu, X., Zhang, M., Zhang, Z., Liu, B., Shi, J., 2025. Cenosphere composite phase change materials in ultra-lightweight foam geopolymer: A pathway to enhance thermophysical and mechanical properties. Constr. Build. Mater. 489, 142053. https://doi.org/10.1016/j.conbuildmat.2025.142053.

Liu, X.Q., Han, Z.X., Luo, Z.L., Lu, H.L., Sun, Y., You, Q., Guo, T.K., Qu, Z.Q., 2024. Sand control mechanism of radial well filled with phase change material in hydrate reservoirs. Pet. Sci. 21, 2571–2582. https://doi.org/10.1016/j.petsci.2024.04.008.

Maiti, M., Bhaumik, A.K., Mandal, A., 2021. Performance of water-based drilling fluids for deepwater and hydrate reservoirs: designing and modelling studies. Pet. Sci. 18, 1709–1728. https://doi.org/10.1016/j.petsci.2021.09.001.

Meng, D., Zhao, K., Wang, A., Wang, B., 2020. Preparation and properties of paraffin/PMMA shape-stabilized phase change material for building thermal energy storage. J. Wuhan Univ. Technol.-Materials Sci. Ed. 35, 231–239. https://doi.org/10.1007/s11595-020-2248-y.

Nazir, H., Batool, M., Ali, M., Kannan, A.M., 2018. Fatty acids based eutectic phase change system for thermal energy storage applications. Appl. Therm. Eng. 142, 466–475. https://doi.org/10.1016/j.applthermaleng.2018.07.025.

Parent, J.S., Bishnoi, P.R., 1996. Investigations into the nucleation behaviour of methane gas hydrates. Chem. Eng. Commun. 144, 51–64. https://doi.org/10.1080/00986449608936444.

Phan, A., Farhadian, A., Iravani, D., et al., 2025. Renewable oilfield reagents with multiple flow-assurance actions: Oleic acid – derived compounds inhibit gas hydrate agglomeration and corrosion. Energy 315, 134368. https://doi.org/10.1016/j.energy.2025.134368.

Shi, J., Tan, J., Liu, B., Liu, Y., Xu, H., Wang, Z., Xiong, T., Shi, J., 2020. Thermal and mechanical properties of thermal energy storage lightweight aggregate mortar incorporated with phase change material. J. Energy Storage 32, 101719. https://doi.org/10.1016/j.est.2020.101719.

Shi, J., Liu, Y., Wang, E., Wang, L., Li, C., Xu, H., Zheng, X., Yuan, Q., 2022. Physico-mechanical, thermal properties and durability of foamed geopolymer concrete containing cenospheres. Constr. Build. Mater. 325, 126841. https://doi.org/10.1016/j.conbuildmat.2022.126841.

Sun, W., Wei, N., Zhao, J., et al., 2022. Imitating possible consequences of drilling through marine hydrate reservoir. Energy 239, 121802. https://doi.org/10.1016/j.energy.2021.121802.

Sun, Y.F., Cao, B.J., Chen, H.N., et al., 2023. Influences of pore fluid on gas production from hydrate-bearing reservoir by depressurization. Pet. Sci. 20, 1238–1246. https://doi.org/10.1016/j.petsci.2022.09.015.

Takeya, S., Hori, A., Hondoh, T., Uchida, T., 2000. Freezing-memory effect of water on nucleation of CO_2 hydrate crystals. J. Phys. Chem. B. 104, 4164–4168. https://doi.org/10.1021/jp993759.

Uchida, T., Yamazaki, K., Gohara, K., 2016. Generation of micro- and nano-bubbles in water by dissociation of gas hydrates. Kor. J. Chem. Eng. 33, 1749–1755. https://doi.org/10.1007/s11814-016-0032-7.

Wang, S., Zhao, X., Wang, Z., Zhang, Y., Wang, H., Zou, D., 2023. Micro-encapsulation of a low-melting-point alloy phase change material and its application in electronic thermal management. J. Clean. Prod. 417, 138058. https://doi.org/10.1016/j.jclepro.2023.138058.

Wei, J., Cheng, Y., Yan, C., Li, Q., Zou, D., Zhang, H., 2019. Drilling parameter optimizing strategies to prevent hydrate decomposition risks. Appl. Therm. Eng. 146, 405–412. https://doi.org/10.1016/j.applthermaleng.2018.09.135.

Xu, Q., Liu, H., Wang, X., Wu, D., 2018. Smart design and construction of nanoflake-like MnO_2/SiO_2 hierarchical microcapsules containing phase change material for in-situ thermal management of supercapacitors. Energy Convers. Manag. 164, 311–328. https://doi.org/10.1016/j.enconman.2018.03.006.

Yan, Q., Wang, W., Yu, D., 2005. An study on phase change materials applied in the building envelope. Mater. Rev. 19, 102–105 (in Chinese).

Yang, L., Zhao, J., Liu, W., Li, Y., Yang, M., Song, Y., 2015. Microstructure observations of natural gas hydrate occurrence in porous media using microfocus X-ray computed tomography. Energy Fuels 29, 4835–4841. https://doi.org/10.1021/acs.energyfuels.5b00881.

Yang, M., Zhao, J., Zheng, J.N., Song, Y., 2019. Hydrate reformation characteristics in natural gas hydrate dissociation process: A review. Appl. Energy. 256, 113878. https://doi.org/10.1016/j.apenergy.2019.113878.

Yin, B., Chen, C., Feng, K., Liu, S., Ren, M., Wang, Z., Sun, B., 2025. Multiphase transient flow in wellbore during shallow hydrate reservoir drilling in deep water. ACS Omega 10, 13701–13714. https://doi.org/10.1021/acsomega.5c01229.

Zhang, L., Zhang, Y., Chen, C., Li, X.S., Chen, Z.Y., 2022. Numerical simulation of hydrate decomposition during the drilling process of the hydrate reservoir in the Northern South China Sea. Energies 15, 3273. https://doi.org/10.3390/en15093273.

Zhang, P., Wu, Q., Mu, C., Chen, X., 2018. Nucleation mechanisms of CO_2 hydrate reflected by gas solubility. Sci. Rep. 8, 10441. https://doi.org/10.1038/s41598-018-28555-y.

Zhang, Y., Su, Y., Ge, X., 1995. Prediction of the melting temperature and the fusion heat of (quasi-) eutectic PCM. J. Univ. Sci. Technol. China. 25, 474–478. https://api.semanticscholar.org/CorpusID:203522106 (in Chinese).

Zhao, J., Yang, Y., Li, Y., Zhao, L., Wang, H., Song, G., Tang, G., 2017. Micro-encapsulated phase change materials with TiO_2-doped PMMA shell for thermal energy storage and UV-shielding. Sol. Energy Mater. Sol. Cells 168, 62–68. https://doi.org/10.1016/j.solmat.2017.04.014.

Zhao, X., Qiu, Z., Zhao, C., Xu, J., Zhang, Y., 2019. Inhibitory effect of water-based drilling fluid on methane hydrate dissociation. Chem. Eng. Sci. 199, 113–122. https://doi.org/10.1016/j.ces.2018.12.057.

Zhao, X., Zhang, X., Li, S., Fang, Q., Qiu, Z., Wang, Z., 2024. Dual function of lecithin as an environmentally-friendly inhibitor of hydrate agglomeration and adhesion to the pipe in gas hydrate production. Fuel 376, 132718. https://doi.org/10.1016/j.fuel.2024.132718.

Zhao, X., Geng, Q., Zhang, Z., et al., 2023. Phase change material microcapsules for smart temperature regulation of drilling fluids for gas hydrate reservoirs. Energy 263, 125715. https://doi.org/10.1016/j.energy.2022.125715.